50th AIAA Aerospace Sciences Meeting including the New Horizons Forum and Aerospace Exposition
09 - 12 January 2012, Nashville, Tennessee

AIAA 2012-0260

MEMS Microphone Array on a Chip for Turbulent Boundary Layer Measurements

Robert D. White[1] and Joshua Krause[2]
Mechanical Engineering, Tufts University, Medford, MA 02155

Richard De Jong[3]
Calvin College, Grand Rapids, MI 49546

and

Gerard Holup[4], Judith Gallman[5], and Mark Moeller[6]
Spirit Aerosystems, Wichita, KS 67210

A MEMS microphone array has been designed and applied to the measurement of wall pressure spectra under the turbulent boundary layer in flow duct testing at Mach numbers from 0 to 0.6. The array was micromachined onto a single chip in the PolyMUMPS surface micromachining process, allowing high spatial resolution and low surface roughness. The chip measures 1 cm by 1 cm, and is flush mounted into the wind tunnel wall. Individual elements are 0.6 mm in diameter, with element to element spacing of 1.11 mm in the crossflow direction and 1.26 mm in the flow direction. The 64 element array has 59 working elements, 58 of which are matched to within ± 2.5 dB at 1 kHz. Phase matching between the 59 elements is ± 6.5 degrees at 1 kHz. The array has been calibrated from 100 Hz to 4 kHz in a plane wave tube. The transducer bandwidth is greater than 400 kHz as determined by laser vibrometry measurements. Sensor nonlinearity of less than 0.36% is observed at a sound pressure level of 150 dB SPL. Board level electronics allow the array to be reconfigured on the fly using computer controlled CMOS switches. Multipoint wall pressure spectra were measured in 38 array configurations at the wall of a 6 inch by 6 inch flow duct at Mach numbers from 0.0 to 0.6. The array shows excellent agreement with Kulite and Bruel & Kjaer microphone measurements in the 300 Hz to 10 kHz band, and appears to be able to measure turbulent pressure spectra at frequencies as high as 40 kHz.

I.   Introduction

THIS paper describes the design, fabrication, characterization, and application of a MEMS microphone array chip for the measurement of wall pressure spectra under turbulent boundary layers (TBL) in wind tunnel testing. The work is motivated by limitations in current wind tunnel instrumentation. In particular, MEMS sensor array-on-a-chip devices allow high spatial resolution by cofabricating multiple array elements side by side on the same die. In addition, MEMS devices allow high bandwidth, high dynamic range, and low surface roughness. These are important characteristics for TBL sensing, since the smallest scales (Kolmogorov scales) of turbulence at the high Reynolds numbers based on plate length ($Re_L \sim 10^6 - 10^7$) typical of subsonic wind tunnels are expected to be on the order of tens of microns [1]. The total sound pressure level in a 20 kHz band can be high. Measurements presented in this work at Mach 0.6 in the 6" x 6" test section of the quiet inlet flow duct exceed 140 dB SPL, and significant energy is seen to be present at frequencies up to 40 kHz. Finally, the law of the wall [2] suggests that at Reynolds

---

[1] Associate Professor, Mechanical Engineering, 200 College Ave, Medford, MA 02155, AIAA Member
[2] Research Assistant, Mechanical Engineering, 200 College Ave, Medford, MA 02155, AIAA Member
[3] Professor, Mechanical Engineering, 3201 Burton St. S.E., Grand Rapids, MI 49546
[4] Acoustic Laboratory Technician, Spirit Aerosystems, 3801 S. Oliver St., Kichita, KS, 67210
[5] Associate Technical Fellow, Spirit Aerosystems, 3801 S. Oliver St., Kichita, KS, 67210, Senior AIAA Member
[6] Acoustic Analyst, Spirit Aerosystems, 3801 S. Oliver St., Kichita, KS, 67210, AIAA Member

numbers based on plate length on the order of 10^6 to 10^7 with free stream velocities of 20 to 200 m/s, the laminar sublayer thickness, which is on the order of 5 wall units, will be approximately 5 to 150 μm thick. In order for the sensor to produce little influence on the flow, the surface roughness should be kept smaller than the laminar sublayer thickness.

Between 1970 and 2000, a number of researchers demonstrated MEMS acoustic sensors and pressure sensors of various types for various applications. Review articles which cover many of these devices include [3-5]. In recent years, a number of MEMS microphones specifically targeted at aeroacoustic applications have been described [6-9]. The sensor chip described in this paper differs from previous MEMS microphone applications in aeroacoustics primarily by fabricating the entire array on a single chip, rather than assembling the array out of individual microphones. This has the advantage of reducing the spacing between elements and may allow better matching of the elements without excessive testing. However, it has the disadvantages of producing a small aperture array, and also does not allow the researcher to discard and replace individual elements that may become damaged.

II. Design and Fabrication

The chip is comprised of 64 individual condenser microphones arrayed on a rectangular grid. The elements themselves consist of a 3.5 micrometer thick, 0.6 mm diameter heavily phosphorus doped polysilicon diaphragm suspended over a 2 micrometer high air gap. Figure 1 shows a diagram of the cross-section. The bottom electrode for the condenser is a 500 nm thick heavily phosphorus doped polysilicon layer which is fabricated directly on a 600 nm thick low stress silicon nitride isolation layer. Below the silicon nitride is a <100> oriented silicon substrate, the surface of which has been heavily doped by phosphorus diffusion. The bottom electrodes of all 64 elements in the array are connected on chip using a 500 nm thick Chrome-Gold metallization layer. The top electrode of each element in the array is wired out to a connection pad along the side of the chip also using the Cr-Au metallization. Guard band lines connected to ground run in between each signal line on chip to reduce element to element capacitive coupling.

Each diaphragm has 28 holes arrayed in a regularly spaced fashion across the surface. The holes are designed to be 4 micrometers in diameter, and serve both as etch holes for the sacrificial etch and vent holes during operation. Control of the hole diameter is critical.   If the holes are too large, the low frequency response of the transducer will be attenuated. If the holes are too small, they may close up and not allow etchant to enter the sacrificial gap, nor allow the device to equalize static pressure across the diaphragm. During micromachining, the holes are defined by plasma etching through the Poly1 and Poly2 layers in the PolyMUMPS process. However, misalignment between the two etches can result in large than desired holes. In order to combat this problem, we coat the diaphragms with Parylene C in post processing. As the Parylene C deposits, it partially closes up the holes. By controlling the length of the Parylene deposition, the hole diameter can be controlled to whatever is needed to achieve the desired low frequency acoustic response, as measured using plane wave tube calibration methods.

In addition, the underside of the diaphragm is covered in dimples, micromachined during the PoylMUMPS process. This helps to reduce stiction of the diaphragm during the release etch. Some diaphragms did fail due to stiction in the drying step after release. However, by drying the elements in a low humidity (<20% RH) environment, stiction problems were avoided.

Fabrication of the chips was conducted through the PolyMUMPS process [MEMSCAP Inc, Durham, North Carolina] and in post processing at the Tufts Micro and
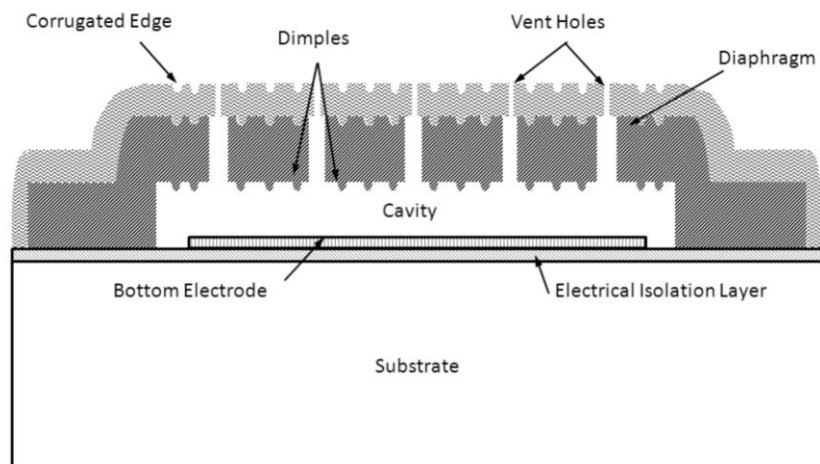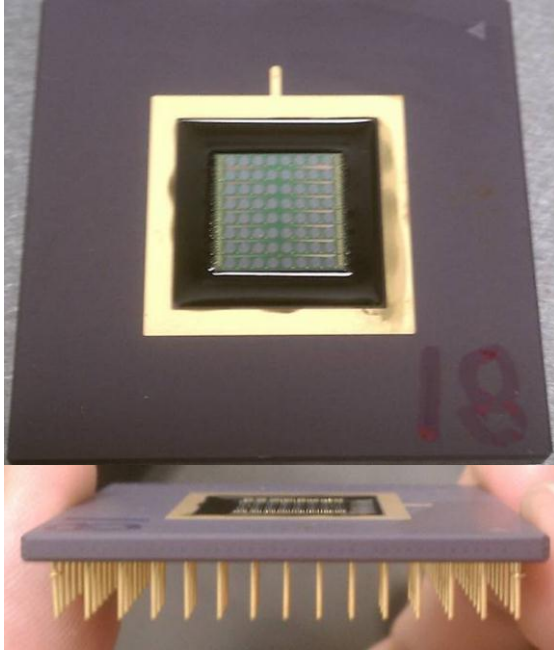
Figure 1. Individual element design.

American Institute of Aeronautics and Astronautics

Figure 2. Photograph of a packaged array chip.

Nano Fabrication Facility. Fabrication has been described previously [10, 11]. Briefly, fabrication begins at Memscap by first depositing the silicon nitride isolation layer, then depositing and patterning of the 600 nm thick polysilicon lower electrode and interconnect layer (Poly0). This is followed by deposition and patterning of the sacrificial phosphosilicate glass layer (Oxide1), including definition of the dimples. This is followed by deposition, patterning, and doping of the two low stress polysilicon layers which make up the 3.5 micrometer thick diaphragm (Poly1 and Poly2). The holes are also patterned into the diaphragm at this step. Finally, the Cr/Au metallization is deposited and patterned. At this point, the wafer is diced and the individual die are shipped to Tufts.

At Tufts, the diaphragm is released using a mixture of 4 parts 49% Hydrofluoric acid (HF) to 1 part 37% Hydrochloric acid (HCl) for 30 minutes. The use of a mixture of HCl and HF rather than straight HF is important. Straight HF attacks the polysilicon grain boundaries, greatly increasing the resistivity of the polysilicon layers. By including HCl in the mixture, this effect can be greatly reduced [12]. After the release etch, the chip is rinsed in water, isopropanol, and methanol, and allowed to air dry in a dry box that has been flooded with clean, dry air with a low relative humidity. By drying in the low humidity environment, stiction problems are reduced.

The chip is next packaged in a ceramic pin grid array hybrid package (CPGA). First, the CPGA cavity is partially filled with potting epoxy [Namics Chipcoat G8345-6] which is cured. The epoxy is then CNC milled to the appropriate height, including a small square pocket to center and align the chip. The chip is mounted into the pocket with a thin epoxy film. This CNC operation sets the height of the chip to ensure that it is centered, aligned, and flush with the top of the package. A thin layer of damming epoxy [Namics Chipcoat G8345D] is painted onto the sides of the die outside the bonding pads in order to reduce shorting problems that can occur if the wirebonds touch the side of the silicon die. The chip is ball bonded to the package using 25 micrometer diameter gold wire. The chip, wirebonds, and package are then coated with Parylene C with a thickness of 1.5 micrometers, for the reasons described above. Finally, the wirebonds are potted in epoxy, which is allowed to settle and cure, with multiple layers being applied until a flat surface is achieved around the chip and package. Using this method, it is possible to create a flat surface with a total maximum topology from the ceramic surface, onto the epoxy, over the wirebonds and onto the chip of approximately 100 micrometers. Figure 2 shows two photographs of a packaged chip.

III. Modeling and Electronics

The computational model for this device has been described previously [10], and follows many of the same methods described by Doody et al. for MEMS cMUT devices[13], with the notable exception that the transducer described here has holes through the diaphragm. A lumped element scheme is adopted as shown in Figure 3, and is valid up to the first resonant frequency at approximately 430 kHz. The
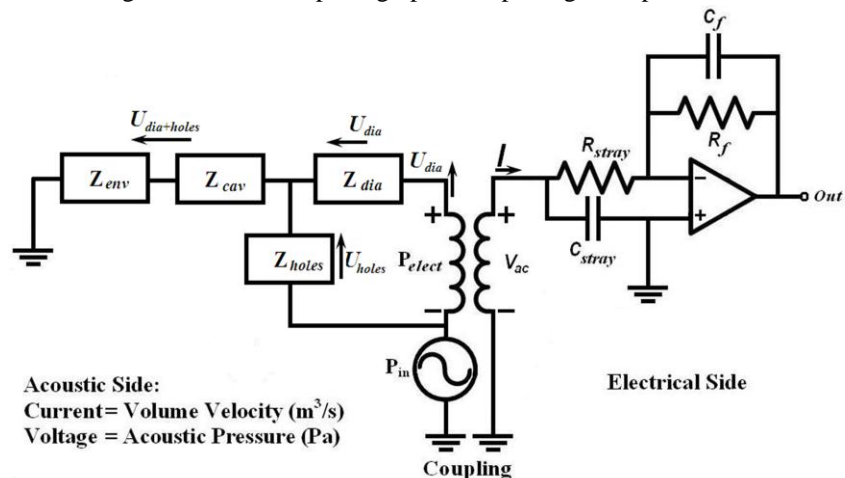

Figure 3. Lumped element model of the single element dynamics.

model includes the laminate plate diaphragm stiffness and mass, Z_{dia}, the acoustic compliance of the backing cavity, Z_{cav}, the damping of the diaphragm holes, Z_{holes}, the acoustic input impedance of the environment for the circular bending modeshape of the transducer, Z_{env}, and electrostatic coupling to the electrical domain. For the details of the various mechanical and acoustic impedances, refer to [10, 13]. The model can be used to compute the output voltage, V_{out}, that is expected for a given fluctuating pressure at the surface of the diaphragm, P_{in}.

The readout electronics, shown in Figure 4, consist of a low noise 10V DC bias source, an array of CMOS switches, two charge amplifiers, and a differential amplifier. In the figure, only two sensors and 6 switches are shown, but that pattern repeats 64 times, once for each sensor. The lower electrode of all the elements is connected to the DC bias source, which can be varied from 0 to 10 V_{dc} with a manual voltage divider. Each top electrode is connected to 3 CMOS switches, one of which is connected to ground, and the other two lead to one of two charge amplifiers. A computer controls the CMOS switches over a serial link, allowing any given microphone in the array to be switched either to ground (off) or switched to one of the two output channels. There are only three analog outputs measured from the board, but the computer can rapidly switch which microphones in the array contribute to each of the outputs. The system is not limited to sending a single microphone to each output; any group of microphones can be switched in parallel to contribute charge to either of the two output channels. The preamps themselves are charge amplifiers constructed from AD795 JFET buffered low noise operational amplifiers with a 47 pF feedback capacitor in parallel with a 50 MΩ resistor. This gives each preamp a charge sensitivity of 21.3 mV/pC at frequencies above 68 Hz. The output of each AD795 preamplifier passes through a high pass filter with a 59 Hz break frequency, and is then gained up by 40 dB by an AD621 instrumentation amplifier before being sent to the output. Measurements of the electronic transfer function indicate that the system achieves 80 dB off isolation. In order to achieve this, it is critical that the microphones that are not being used be switched to ground, rather than simply left floating. This architecture for the electronics has the advantage that the array can be rapidly reconfigured, allowing the sensor chip to rapidly switch between different effective apertures, and yet only two analog output lines and two preamplifiers are needed. Since the preamplifiers are the major source of electronic noise in the system, this greatly improves the signal to noise ratio compared to what would be experienced by a system with a separate preamplifier for each microphone. In addition, since only two preamplifiers are present, it is much easier to match the amplifier frequency responses than if there were 64 separate preamplifiers. However, the disadvantage of this architecture is that complete beam-forming is not possible, as each microphone signal cannot be access individually at the same time.
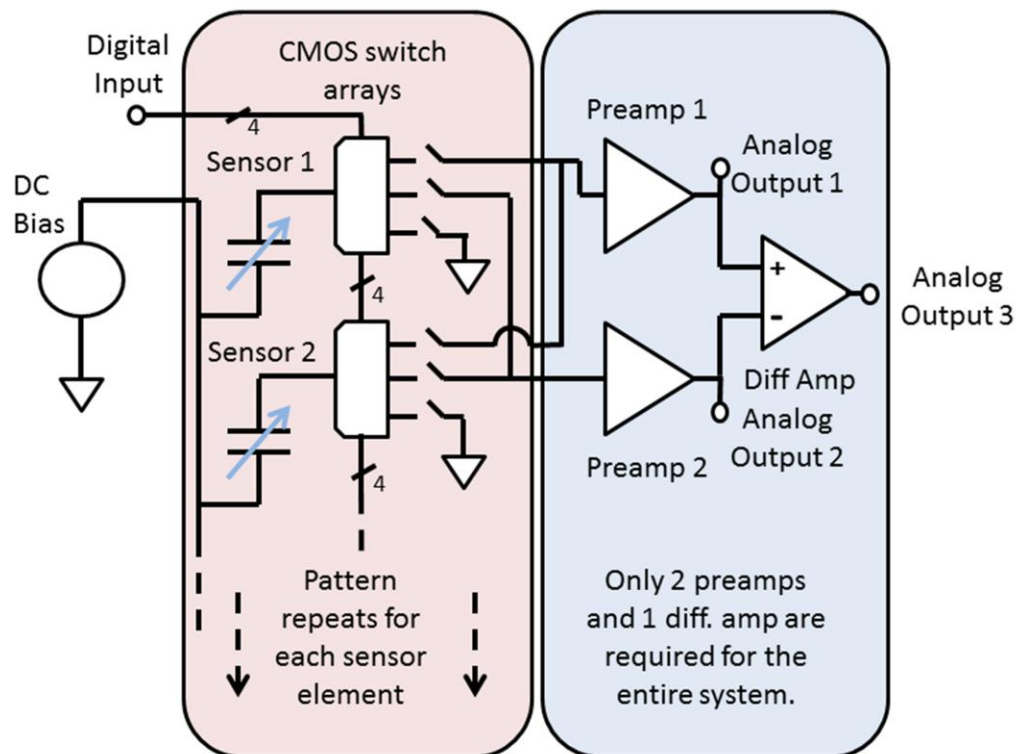

Figure 4. Readout electronics for the sensor chip.

American Institute of Aeronautics and Astronautics

Downloaded by Robert White on March 26, 2013 | http://arc.aiaa.org | DOI: 10.2514/6.2012-260

IV. Calibration

The MEMS array has been tested acoustically in a plane wave tube with a ¼" Bruel & Kjaer microphone mounted flush in the tube directly across from the MEMS array. The tube is ½" square, resulting in a non-plane mode cutoff frequency of 11 kHz. The tube is driven by an acoustic driver and rigidly terminated, so a standing wave develops in the tube. The test location is approximately 2 cm from the end of the tube, so the first pressure null in the standing wave field reaches the test location at a frequency of approximately 4 kHz. This feature is clearly seen in the acoustic calibration results of Figure 5, and sets the upper frequency at which the device can be calibrated using this apparatus. Figure 5 shows results for each of the 59 working elements in the array. The sensitivity in the mid band is between 0.1 mV/Pa and 0.25 mV/Pa. With the exception of one outlier (with a slightly higher sensitivity that the other 58 microphones), sensitivity between the elements varies by ± 2.5 dB at 1 kHz. Phase variation among all 59 elements is ± 6.5 degrees at 1 kHz. The measured sensitivity is an almost perfect match to model predictions, shown as the dotted line in Figure 5. Individual microphones cannot be calibrated below 300 Hz in this setup because the individual microphone signal to noise ratio (SNR) is too low. However, by switching all the elements in the array to one amplifier, the sensitivity essentially increases by a factor of 59 while the noisefloor stays fairly constant. A measurement of this type (not shown) has been conducted and shows a smooth frequency response down to 100 Hz, in good agreement with the model. Some reduction in sensitivity is seen at low frequencies; the half power frequency is approximately 200 Hz.

Laser vibrometer measurements shown elsewhere [10] indicate that the first resonant frequency of the microphone is greater than 400 kHz, suggesting that the microphones can be used at frequencies up to 400 kHz, although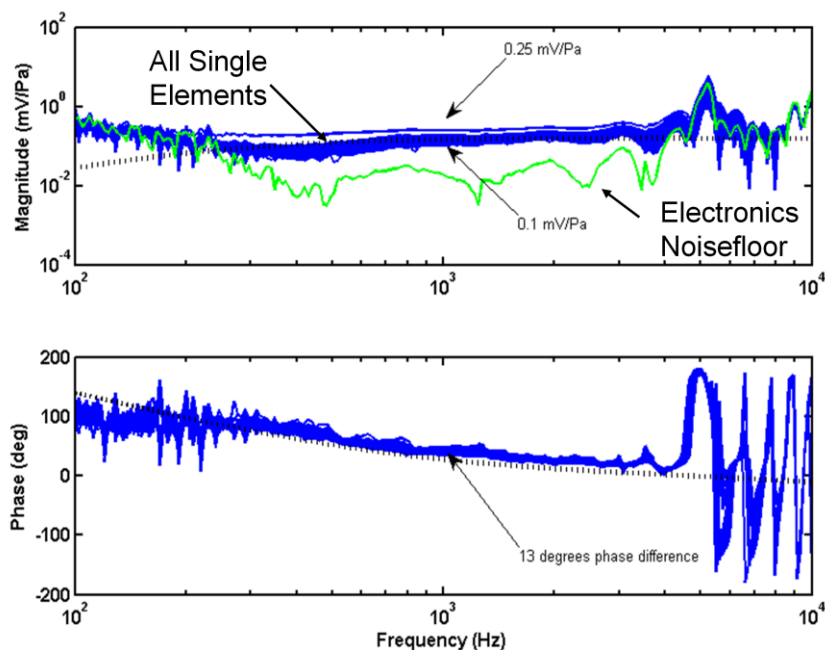 this has not been confirmed by acoustic calibration. The bandwidth of the electronics sets the upper limit of operation of the current system at 40 kHz, although this could be increased with minor changes to the electronics.

In preparation for flow duct testing, the array was calibrated using this method for each of the 38 different configurations that were used in the flow duct. A complete calibration curve was generated by using the measured results in the 300 Hz – 4 kHz band, and then extrapolating these results to extend from low frequencies (< 1 Hz) to high frequencies (> 40 kHz).

Figure 5. Acoustic calibration of all 59 working elements in the MEMS array compared to a ¼" B&K reference microphone.

V. Flow Duct Testing

The MEMS array was flush mounted into an aluminum plate on the 6 inch by 6 inch quiet inlet flow duct at Spirit Aerosystems. The flow duct has been described in detail elsewhere, including acoustic and turbulence measurements using pitot probes, hot wire anemometers, and kulite high intensity microphones [14, 15]. The duct has been acoustically treated to reduce the facility acoustic noise as much as possible, including careful design of the mixer, diffuser, and nozzle, although measurements show that acoustic noise still dominates turbulent pressures at the wall for frequencies below approximately 400 Hz [15]. The system also includes a settling chamber and screens for straightening the flow and reducing turbulent intensity in the flow that enters the test section. The test section itself has a square 6" x 6" cross section and extends 22 feet from the contraction section to the diffusion section and exhausts into the environment. The system is capable of achieving Mach numbers from 0 to 0.6.

5

American Institute of Aeronautics and Astronautics

In addition to two channels of measurements taken by the MEMS array, instrumentation in the flow duct tests included four kulite high intensity microphones, style MIC-093 [Kulite Semiconductor Products, Leonia, NJ], a Bruel & Kjaer Type 4136 ¼" condenser microphone [Bruel & Kjaer, Naerum, Denmark], and a Dytran 3225E1 miniature accelerometer [Dytran Instruments Inc, Chatsworth, CA] for measuring structural vibrations. All eight channels were sampled at 120 kHz for 1 second in each of thirty eight array configurations. Tests were run at six Mach numbers from 0.1 to 0.6 Ma, as well as a test with no flow.

Data analysis is still ongoing and will be more completely described in the full paper. Briefly, the 38 configurations were selected to investigate the effects of the following on single-point or two-point wall pressure spectra: (1) sensor effective aperture (2) distance between transducers (3) downstream wavenumber (4) cross stream wavenumber (5) bidirectional wavenumber. Since two measurements are captures simultaneously, it is possible to examine cross-spectra (phase and coherence) as well as single point power spectra. The time domain data was analyzed using 8192 point 50% overlapping Hanning windowed sections to produce averaged power spectra and crossspectra. Figure 6 shows some of the data.
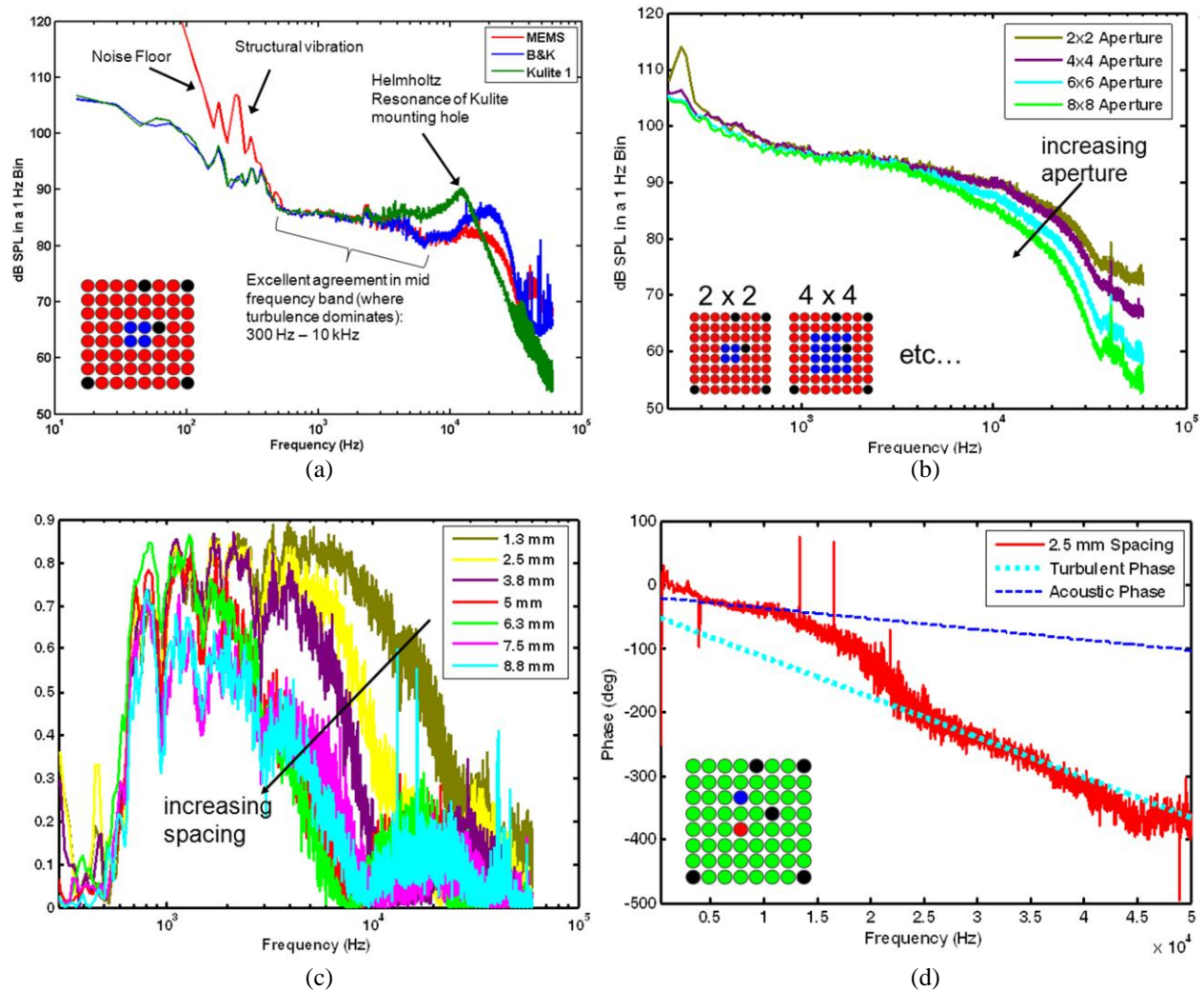

(a)

(b)

(c)

(d)

Figure 6. Flow duct spectra. (a) Comparison between the power spectra of a 2x2 MEMS array, a B&K 4136 microphone and a Kulite high intensity microphone at Mach 0.3 . (b) Comparison of the power spectra for MEMS array apertures of different size from 2x2 to 8x8 at Mach 0.6. (c) Comparison of the coherence between two individual MEMS microphones at different downstream center-to-center distances at Mach 0.6. (d) The phase difference between two individual MEMS microphones at a downstream distance of 2.5 mm at Mach 0.6.

6

American Institute of Aeronautics and Astronautics

Figure 6 (a) shows a comparison between the power spectra measured with a 2 x 2 array of MEMS microphones to that measured by the B&K 4136 and a kulite at Mach 0.3. In the mid frequency band between 300 Hz and 2 kHz, all three sensors agree very well. Between 2 kHz and 10 kHz, we still see excellent agreement between the MEMS sensor and the B&K microphone. The kulite shows a higher spectral level in the 2-10 kHz band, peaking at approximately 12 kHz. This is thought to be the Helmholtz resonance of the kulite mounting hole, since the kulite is mounted in a pinhole. The good agreement between the sensors lends considerable confidence to the MEMS measurements. Since the MEMS microphones are not mounted in a pinhole, have almost no surface topology or windscreens, and are flush with the duct surface, as well as having a flat frequency response out to 40 kHz, we are inclined to believe the MEMS data over the B&K data in the 10 kHz – 40 kHz band, although further analysis needs to be done.

Figure 6 (b) shows the result of changing the aperture of the MEMS array from 2 x 2 (1.11 mm x 1.25 mm center to center pitch) to 8 x 8 at Mach 0.6. As the aperture increases, the measured pressure spectra at frequencies from 5-40 kHz is seen to decrease. This suggests that the high temporal frequency components of the wall pressure spectra exhibit high wavenumbers, and thus are averaged out by the larger apertures. This is expected, as the turbulent wall pressure fluctuations are expected to have significant energy at high spatial wavenumbers. Further analysis is needed to compare this result to established turbulence models.

Figure 6 (c) shows the coherence between two individual MEMS microphones as the downstream distance between them is increased at Mach 0.6. If the wall pressure is primarily turbulent, we would expect the coherence to decrease significantly over distances of the same order as the thickness of the boundary layer. In the data, we see that the coherence is high for all spacing at frequencies from about 500 Hz to about 2 kHz. This suggest that in this band, the major contributor to the wall pressure spectra is acoustic. However, at frequencies from 2 kHz to 40 kHz, we see that at small spacings (1.3 mm) coherence is high, but as spacing increases, coherence rapidly drops. There appears to be a particularly rapid drop in coherence between 3.8 mm and 5 mm spacing, which is a spacing that is on the same order as the boundary layer thickness for this flow speed.

Figure 6 (d) shows the phase between two individual MEMS microphones spaced 2.5 mm apart downstream at Mach 0.6. The measured phase is compared to the acoustic phase (computed using the sum of the speed of sound and the free stream velocity) and to the expected phase for coherent structures convecting as turbulence with a speed equal to 70% of the free stream velocity. It is seen that at frequencies above 20 kHz, the phase matches the expected turbulent phase very closely, while at frequencies below 15 kHz the phase speed is somewhere between the acoustic and turbulent convection speeds. This suggests that above 20 kHz, turbulent pressures dominate the wall pressure spectra. However, it is unclear what is causing the intermediate phase speed at lower frequencies.

All microphones in the MEMS array survived testing at the full range of Mach numbers.

VI. Conclusions

A fronted vented, 64 element MEMS microphone array on a chip has been designed and demonstrated for aeroacoustic measurements in a flow duct. The array achieves high spatial resolution of 1.1 to 1.25 mm center to center spacing of the elements with individual element diameters of 0.6 mm. Calibration curves were collected in a plane wave tube for a variety of array configurations, and allow the array to be used for single point and two-point wall pressure spectra measurements under the TBL from 100 Hz to 40 kHz. With a minor redesign of the electronics, the bandwidth could be extended as high as 400 kHz.

The electronics for the system uses a unique CMOS switch architecture to rapidly reconfigure the array on the fly, allowing for a variety of tests to be performed. The array was integrated into a 6 inch square flow duct test facility and used to measure wall pressure spectra under the TBL at Mach 0 to 0.6. Excellent agreement was found between the MEMS array and both B&K and kulite sensors at frequencies from 300 Hz to 2 kHz. At higher frequencies, some differences were seen between the sensors. The MEMS array may be out-performing the larger sensors at high frequencies, although further analysis is needed to confirm this.

Preliminary analysis of flow duct data shows the presence of both acoustic and turbulent components to the wall pressure spectra. Sensor effective aperture is shown to affect spectral measurements at frequencies above 5 kHz. A

sensor of less than approximately 3 to 4 mm in diameter is needed to fully resolve the spectral content at frequencies above 10 kHz. The coherence between two points is shown to decrease with distance over the 1.3 to 5 mm range at frequencies above 2 kHz, suggesting that turbulence plays a major role at these frequencies for the measured flow conditions. This is also borne out by phase measurements, although further analysis is needed. Additional analysis of the full data set will be presented at the meeting and in the full paper.

References

1. Lofdahl, L., and Gad-el-Hak, M. "MEMS-based pressure and shear stress sensors for turbulent flows," *Measurement Science & Technology* Vol. 10, 1999, pp. 665-686.
2. Fay, J. A. *Introduction to fluid mechanics*: The MIT Press, 1994.
3. Lofdahl, L., and Gad-el-Hak, M. "MEMS applications in turbulence and flow control," *Progress in Aerospace Sciences* Vol. 35, No. 2, 1999, pp. 101-203.
4. Scheeper, P. R., van der Donk, A. G. H., Olthuis, W., and Bergveld, P. "A review of silicon microphones," *Sensors and Actuators A: Physical* Vol. 44, No. 1, 1994, pp. 1-11.
5. Sessler, G. M. "Acoustic sensors," *Sensors and Actuators A: Physical* Vol. 26, No. 1-3, 1991, pp. 323-330.
6. Horowitz, S., Nishida, T., Cattafesta, L., and Sheplak, M. "Development of a micromachined piezoelectric microphone for aeroacoustics applications," *Journal of the Acoustical Society of America* Vol. 122, No. 6, 2007, pp. 3428-3436.
7. Martin, D. T., Liu, J., Kadirvel, K., Fox, R. M., Sheplak, M., and Nishida, T. "A micromachined dual-backplate capacitive microphone for aeroacoustic measurements," *Journal of Microelectromechanical Systems* Vol. 16, No. 6, 2007, pp. 1289-1302.
8. Williams, M. D., Griffin, B. A., Meloy, J., and Sheplak, M. "A microelectromechanical systems-based piezoelectric microphone for aeroacoustic measurements," *The Journal of the Acoustical Society of America* Vol. 128, No. 4, 2010, p. 2444.
9. Wetzel, D., Bahr, C., Williams, M., Meloy, J., Sheplak, M., and Cattafesta, L. "An aeroacoustic microelectromechanical systems microphone phased array," *The Journal of the Acoustical Society of America* Vol. 129, 2011, p. 2645.
10. Krause, J. S., White, R. D., Moeller, M. J., and De Jong, R. "MEMS pressure sensor array for aeroacoustic analysis of the turbulent boundary layer," *Aerospace Sciences Meeting*. Orlando, 2009.
11. Carter, J., Cowen, A., Hardy, B., Mahadevan, R., Stonefield, M., and Wilcenski, S. "PolyMUMPs Design Handbook: a MUMPs process." 2005.
12. Miller, D. C., Hughes, W. L., Wang, Z.-L., Gall, K., and Stoldt, C. R. "Mechanical Effects of Galvanic Corrosion on Structural Polysilicon," *Microelectromechanical Systems, Journal of* Vol. 16, No. 1, 2007, pp. 87-101.
13. Doody, C. B., Xiaoyang, C., Rich, C. A., Lemmerhirt, D. F., and White, R. D. "Modeling and Characterization of CMOS-Fabricated Capacitive Micromachined Ultrasound Transducers," *Microelectromechanical Systems, Journal of* Vol. 20, No. 1, 2011, pp. 104-118.
14. Miller, T. S., Gallman, J. M., and Moeller, M. J. "Investigation of Low-Frequency Single Point Wall Pressure Spectrums," *17th AIAA/CEAS Aeroacoustics Conference (32nd AIAA Aeroacoustics Conference)*. Portland, Oregon, 2011.
15. Miller, T. S., Lee, S. W., Holup, G., Gallman, J. M., and Moeller, M. J. "Design of a Quiet Inlet for a 6x6 Boundary Layer Flow Duct," *the SAE 2011 Noise and Vibration Conference and Exhibition*. Grand Rapids, 2011.